ChemPubSoc Europe

DOI: 10.1002/open.201800044

Open Access ChemistryOPEN Communications

Exploring the Interactions of Oxygen with Defective ZnO

Xuan Wang[+],[a, b] Bin Lu[+],[a, c] Ling Li,[a, b] and Hengshan Qiu*[a]

Exploring the interactions of oxygen with defective oxide is of importance to understand the microscopic process and performance of ZnO-based oxygen sensors. The interactions of environmental oxygen with vacuum-annealed defective ZnO have been studied by electrical methods, vacuum Fourier transform infrared spectroscopy, and in situ adsorption experiments. It was found that the vacuum-annealed defective ZnO exhibits varied electrical response at different temperatures, which, by vacuum IR investigation, was ascribed to the subtle balance between formation of oxygen vacancies and their interactions with environmental oxygen. Further studies showed that two microscopic steps including surface adsorption and bulk diffusion were dominating the interactions between defective ZnO and environmental oxygen, and the corresponding apparent activation energies were estimated to be 0.093 and 0.67 eV through in situ adsorption experiments. The quite low activation barrier of oxygen adsorption on the defective ZnO was proposed to be responsible for the extreme high sensitivity of ZnO-based oxygen sensors.

Oxygen vacancies have been frequently considered as a key factor in determining the physicochemical properties of gas sensors, catalysts, solar cells, semiconductors, and so forth.[1] Specifically, the oxygen vacancies were proposed to be the active sites on the ZnO-based catalysts for methanol synthesis.[2] The green emission in ZnO phosphors has been ascribed to the recombination of a photogenerated hole with the singly ionized charge state at oxygen vacancies.[3] Moreover, in several research works, the defective ZnO was reported to be far superior to the stoichiometric one as oxygen sensors.[4] The formation, concentration, and migration properties of oxygen vacancies have been studied theoretically and experimentally.[5] However, a thorough understanding of the interactions of defective ZnO with environmental oxygen is still scarce. In this work, we reported a varied electrical response of vacuum-annealed ZnO nanoparticles to environmental oxygen at different temperatures and studied the microscopic interactions between oxygen and vacuum-annealed defective ZnO by using vacuum Fourier transform infrared (FTIR) spectroscopy and adsorption methods. The varied electrical response was ascribed to the subtle balance between the formation of oxygen vacancies (including surface and bulk vacancies) and adsorption/diffusion of oxygen.

To measure the electrical response to environmental oxygen, the as-prepared ZnO sample was annealed under vacuum at 643 K for 2 h. The electrical response to 0.1 mbar oxygen was then measured at 323 and 623 K, respectively, as shown in Figure 1. It can be clearly seen from the Figure 1 A that the current decreases abruptly by more than two orders of magnitude when exposed to 0.1 mbar oxygen. Analysis shows that the current reaches a third of the maximum value within 10 s, exhibiting an extremely fast response. The current does not recover after evacuating the O_2, which indicates an irreversible change of the sample during response to environmental oxygen at 323 K. Figure 1 B shows the electrical response at 623 K during the repeated oxygen-in (introduction) and oxygen-out (evacuation) cycles. Interestingly, the current can be recovered within 2 h under high vacuum at 623 K. The disparate electrical response, after straightforward speculation, comes from the different vacancy formation kinetics at different temperatures. This speculation was further confirmed by our test data, showing that an elevated temperature can effectively reduce the recovery time (e.g. a recovery time less than 20 min was obtained at 673 K under high vacuum). Indeed, the importance of oxygen vacancies has been often emphasized in ZnO-based oxygen sensors. It has also long been thought that the intrinsic n-type conductivity of as-prepared ZnO can be attributed to the presence of either hydrogen[6] or oxygen vacancies in ZnO bulk,[7] which usually give rise to shallow donor states. As a result, electrons at donor levels can be thermally excited to the conduction band of ZnO and become free charge carriers.

To verify such a proposed model, vacuum-transmission FTIR experiments have been performed on the ZnO nanoparticles to investigate the IR absorption of free charge carriers (see Section I of the Supporting Information for a detailed descrip-

[a] X. Wang,[+] B. Lu,[+] L. Li, Prof. H. Qiu
Laboratory of Environmental Science and Technology
Xinjiang Technical Institute of Physics & Chemistry
Key Laboratory of Functional Materials and
Devices for Special Environments
Chinese Academy of Sciences
Urumqi 830011 (P. R. China)
E-mail: qiu@ms.xjb.ac.cn

[b] X. Wang,[+] L. Li
University of Chinese Academy of Sciences
Beijing 100049 (P. R. China)

[c] B. Lu[+]
State Key Laboratory of Silicate Materials for Architectures
School of Materials Science and Engineering
Wuhan University of Technology
Wuhan 430070 (P. R. China)

[+] These authors contributed equally to this work

Supporting Information and the ORCID identification number(s) for the author(s) of this article can be found under: https://doi.org/10.1002/open.201800044.

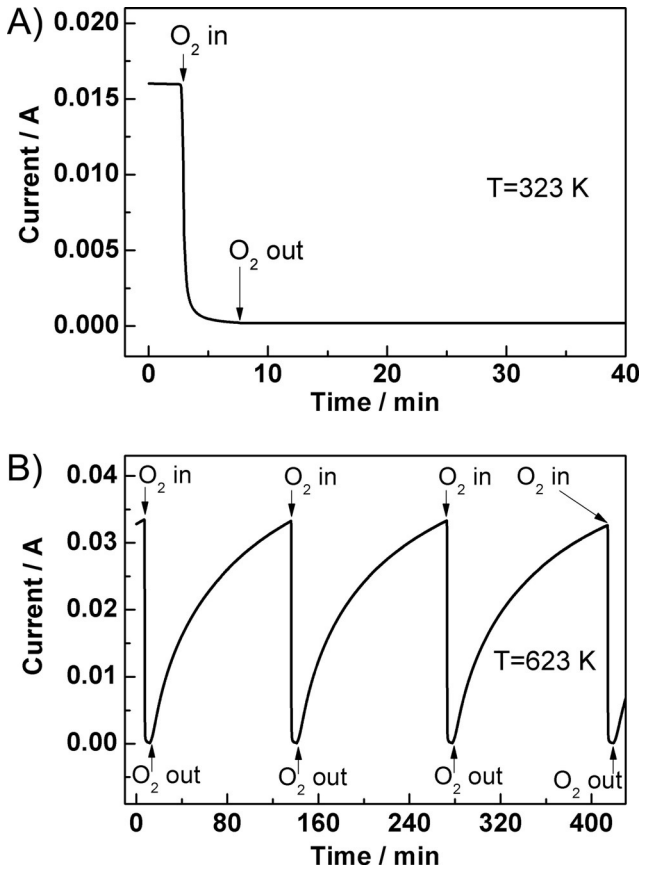

Figure 1. The electrical response of vacuum-annealed ZnO under an environmental oxygen pressure of 0.1 mbar measured at A) 323 K and B) 623 K. Before each experiment, the ZnO sample was annealed at 643 K in high vacuum for 2 h.

tion).[8] Before IR experiments, the sample was evacuated for 2 h and annealed at 850 K for 20 min to remove surface contamination. The sample was then oxidized at 850 K under 10^{-4} mbar oxygen for 10 min. Figure 2A shows the ZnO spectra after annealing at 643 K under high vacuum for different lengths of time. The reference spectrum was taken on clean ZnO at room temperature (RT). With increasing annealing time, the ZnO spectra gradually shift to a higher position, indicating an increase in absorption of IR light. Indeed, this phenomenon has been used to study the hydrogen doping effect in bulk ZnO and ascribed to the IR absorption of free charge carriers.[9] By using typical parameters for ZnO (see Section II of the Supporting Information for details), the value of the concentration of free charge carriers in ZnO was calculated to be 2.9×10^{15} cm^{-3}. If we use this value to estimate the electrical resistivity of the vacuum-annealed ZnO, a value of 1.26 Ω·m is obtained (see Section II of the Supporting Information), which is in good agreement with the experimental value of 0.47 Ω·m measured by the electrical method adopted in Figure 1. Figure 2B presents the IR spectra of the vacuum-annealed ZnO under different oxygen pressures. The reference spectrum was taken on the vacuum-annealed sample in Figure 2A. With elevating oxygen pressures, the IR absorption spectra gradually shift to lower positions, indicating a decrease in charge carrier

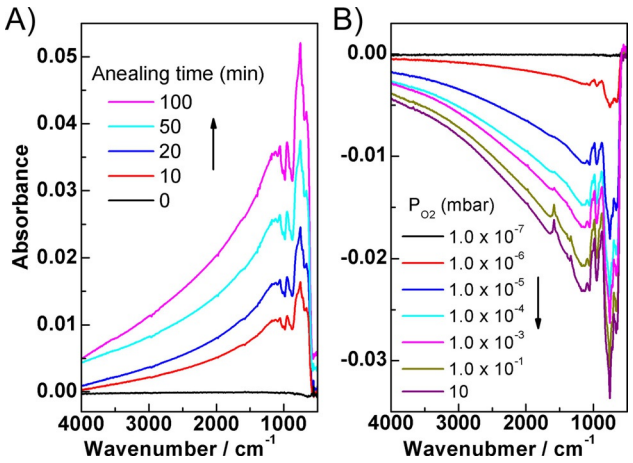

Figure 2. A) Transmission IR spectra of the ZnO sample after annealing at 643 K under high vacuum for different lengths of time. The reference spectrum was taken on a clean ZnO sample. A) Transmission IR spectra of the vacuum-annealed sample were exposed to oxygen with different pressures, P_{O_2}. The reference spectrum was taken on the vacuum-annealed sample in (A).

concentration of ZnO. The IR experiments demonstrated that the concentration of free charge carriers is significantly influenced by both temperature and environmental oxygen pressure.

In Figure 3, the temperature- and oxygen-pressure-dependent electrical responses are presented. At higher temperatures (i.e. above 523 K), the currents decrease monotonically with increasing oxygen pressure, indicating that equilibrium was reached between losses and supplements of oxygen in the ZnO sample at different oxygen pressures. At lower temperatures (i.e. below 423 K), the response curves exhibit similar behaviors to those of the high-temperature curves at lower oxygen pressure. However, a plateau appears at around 0.01 mbar, which indicates saturation conditions. In other words, no more oxygen can be supplied to the ZnO sample above 0.01 mbar at lower-temperature conditions. Interestingly, the high-temperature curves cross the low-temperature curves at around 1 mbar and reach a low value at 10 mbar.

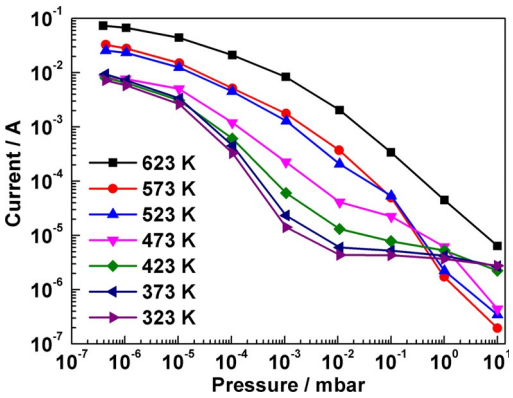

Figure 3. The electrical response of vacuum-annealed ZnO under the indicated temperature and environmental oxygen pressure. Before each experiment, the ZnO sample was annealed at 643 K under high vacuum for 2 h.

Note that, because higher temperatures excite more electrons in the donor level to the conduction band, a higher response current will be achieved for a same density of donor states at higher temperatures.[6b] The emergence of the crossover, therefore, implies that more oxygen can be supplied to the defective ZnO at higher temperature. This phenomenon strongly suggests that two processes with different activation energies are involved to supply oxygen: a surface adsorption process with a lower activation barrier and bulk diffusion with a higher activation barrier. The plateau in the low-temperature curves is then explained by the saturation of surface adsorption and the crossover is the consequence of bulk diffusion. In addition, the different behaviors of the 623 K curve indicates that the out-diffusion of oxygen starts to show a nonnegligible effect on the equilibrium condition at this temperature, which is consistent with previous work showing that irradiation-induced defects fully recover after annealing at 600 K.[10]

To estimate the activation barriers of the two processes, in situ adsorption of oxygen was carried out (see Section III of the Supporting Information). The ZnO sample was annealed at 643 K for 4 h under a pressure of 10^{-3} mbar before oxygen adsorption. Figure 4 shows the adsorption curves of oxygen at different temperatures. The curves decrease dramatically in the first few seconds (see the inset) and then gradually decrease. Two segments with remarkably different decreasing rates are ascribed to the surface adsorption and bulk diffusion processes. After 40 min, only the 623 K curve reaches equilibrium, indicating limited out-diffusion and a desorption rate of the oxygen below 623 K, which is in good agreement with Figure 3. We, therefore, take the maximum pressure change in the figure (the point at 2400 s on the 573 K curve) to estimate the concentration of oxygen vacancies in ZnO bulk, which is calculated to be 1.40×10^{20} cm^{-3} (see Section III of the Supporting Information). By using the value for the concentration of oxygen in stoichiometric ZnO of 4.146×10^{22} cm^{-3}, the oxygen vacancies amounts to 0.34% in bulk ZnO. The adsorption and diffusion rates are estimated from the slopes in the initial seconds for surface adsorption and at 460 Pa (which results in the same bulk concentration of oxygen vacancies) for bulk diffusion.

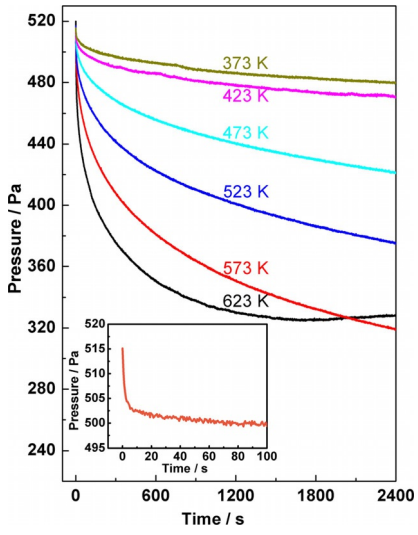

Figure 4. In situ adsorption of oxygen on vacuum-annealed ZnO at the indicated temperature. Before the experiment, the ZnO sample was annealed at 643 K under vacuum for 2 h.

Figure 5 shows the Arrhenius plots for the adsorption and diffusion processes. The apparent activation barriers for surface adsorption and bulk diffusion were estimated to be 0.093 and 0.67 eV, respectively. The reasonable low activation barrier for surface adsorption of oxygen on ZnO is responsible for the extremely fast and sensitive electrical response to environmental oxygen partial pressure. The activation barrier of bulk diffusion is much smaller than the calculated diffusion barrier of oxygen vacancies in ZnO bulk,[5a,d] indicating that the existence of oxygen vacancies in ZnO bulk significantly reduces the diffusion barrier of oxygen.

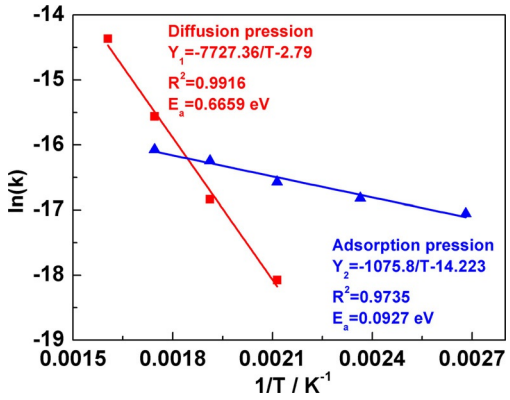

Figure 5. Arrhenius plot of the oxygen adsorption and diffusion on the vacuum-annealed ZnO.

In conclusion, the varied electrical responses of vacuum-annealed defective ZnO under different environmental oxygen partial pressures and temperatures were correlated with the subtle balance between the formation of oxygen vacancies and their interactions with environmental oxygen (surface adsorption and bulk diffusion). The extremely high sensitivity originates from the low activation barrier of oxygen adsorption on defective ZnO. This work provides a way to approximately estimate the performance and stability of oxygen sensors. In addition, as many physicochemical properties of material are determined through oxygen vacancies, it indicates that much more attention should be paid to the environment of the material being exposed, for example O-rich or O-lean conditions at different temperatures, for ZnO-based materials and, more generally, oxide materials. It also suggests that ex situ characterization in a traditional way may not always represent the real situation, whereas in situ investigation under reaction conditions may describe a thorough scenario.

Experimental Section

The ZnO nanoparticles used in this work were supplied by Sigma–Aldrich Corp. with an average size smaller than 100 nm. For the

electrical measurements, ZnO nanoparticles were first dispersed in water and then coated onto an interdigital electrode. After drying in air, the interdigital electrode was fixed on a heating plate and put in a high vacuum chamber with the base pressure above 6×10^{-8} mbar. Two terminals of the electrode were led out through two isolated electrical feedthroughs. The electrical measurement was carried out with a source meter (Keithley 2636B) at a bias voltage of 0.5 V. The IR experiments were performed with a modified vacuum FTIR spectrometer (Bruker Vertex 70v). The base pressure in the spectrometer was 0.1 mbar and in the IR chamber was 2×10^{-7} mbar (see Section I of the Supporting Information for a detailed description).[8] In all experiments, a pressure lower than 10^{-2} mbar was read from a full-range vacuum gauge and those above 10^{-2} mbar were recorded by capacitance gauges.

Acknowledgements

This project was supported by the National Natural Science Foundation of China (Project No. 21373267), Project of Development of Scientific Equipment, CAS (Project No. yz201451), and the 1000-Talent Program (Recruitment Program of Global Expert).

Conflict of Interest

The authors declare no conflict of interest.

Keywords: activation energy · adsorption · bulk diffusion · defective ZnO · sensors

[1] a) K. Hashimoto, H. Irie, A. Fujishima, *Jpn. J. Appl. Phys.* **2005**, *44*, 8269 – 8285; b) G. Sedmak, S. Hočevar, J. Levec, *J. Catal.* **2003**, *213*, 135 – 150; c) C. Soci, A. Zhang, B. Xiang, S. A. Dayeh, D. P. R. Aplin, J. Park, X. Bao, Y. H. Lo, D. Wang, *Nano Lett.* **2007**, *7*, 1003 – 1009; d) Q. Wan, Q. Li, Y. Chen, T. Wang, X. He, J. Li, C. Lin, *Appl. Phys. Lett.* **2004**, *84*, 3654 – 3656; e) H. Qiu, H. Idriss, Y. Wang, C. Wöll, *J. Phys. Chem. C* **2008**, *112*, 9828 – 9834.

[2] a) M. Kurtz, J. Strunk, O. Hinrichsen, M. Muhler, K. Fink, B. Meyer, C. Wöll, *Angew. Chem. Int. Ed.* **2005**, *44*, 2790 – 2794; *Angew. Chem.* **2005**, *117*, 2850 – 2854; b) M. Kurtz, J. S. Dipl. -Chem, O. Hinrichsen, M. Muhler, K. Fink, B. Meyer, C. Wöll, *Angew. Chem. Angewandte Chemie* **2005**, *117*, 2850 – 2854; c) J. Kiss, D. Langenberg, D. Silber, F. Traeger, L. Jin, H. Qiu, Y. Wang, B. Meyer, C. Woll, *J. Phys. Chem. A* **2011**, *115*, 7180 – 7188.

[3] K. Vanheusden, W. L. Warren, C. H. Seager, D. R. Tallant, J. A. Voigt, *J. Appl. Phys.* **1996**, *79*, 7983 – 7990.

[4] a) Y. Yan, M. M. Al-Jassim, S.-H. Wei, *Phys. Rev. B* **2005**, *72*, 161307; b) J. C. Yen, *J. Vac. Sci. Technol.* **1975**, *12*, 47 – 51; c) V. Kobrinsky, A. Rothschild, V. Lumelsky, Y. Komem, Y. Lifshitz, *Appl. Phys. Lett.* **2008**, *93*, 113502 – 113504; d) T. Goto, Y. Shimizu, H. Yasuda, T. Ito, *Appl. Phys. Lett.* **2016**, *109*, 0231041 – 0231044.

[5] a) B. Deng, A. Luisa da Rosa, T. Frauenheim, J. P. Xiao, X. Q. Shi, R. Q. Zhang, M. A. Van Hove, *Nanoscale* **2014**, *6*, 11882 – 11886; b) V. Ischenko, S. Polarz, D. Grote, V. Stavarache, K. Fink, M. Driess, *Adv. Funct. Mater.* **2005**, *15*, 1945 – 1954; c) A. Janotti, C. G. Van de Walle, *Appl. Phys. Lett.* **2005**, *87*, 122102; d) A. Janotti, C. G. Van de Walle, *Phys. Rev. B* **2007**, *76*, 165202.

[6] a) D. M. Hofmann, A. Hofstaetter, F. Leiter, H. Zhou, F. Henecker, B. K. Meyer, S. B. Orlinskii, J. Schmidt, *Phys. Rev. Lett.* **2002**, *88*, 045504; b) H. Qiu, B. Meyer, Y. Wang, C. Wöll, *Phys. Rev. Lett.* **2008**, *101*, 236401; c) G. A. Shi, M. Saboktakin, M. Stavola, *Appl. Phys. Lett.* **2004**, *85*, 5601 – 5603.

[7] a) L. E. Halliburton, N. C. Giles, N. Y. Garces, M. Luo, C. Xu, L. Bai, L. A. Boatner, *Appl. Phys. Lett.* **2005**, *87*, 172108; b) F. Leiter, H. Alves, D. Pfisterer, N. G. Romanov, D. M. Hofmann, B. K. Meyer, *Physica B* **2003**, *340 – 342*, 201 – 204; c) W. L. Bond, *J. Appl. Phys.* **1965**, *36*, 1674 – 1677.

[8] Y. Du, L. Li, X. Wang, H. Qiu, *Appl. Spectrosc.* **2018**, *72*, 122 – 128.

[9] a) H. Noei, H. Qiu, Y. Wang, M. Muhler, C. Woll, *ChemPhysChem* **2010**, *11*, 3604 – 3607; b) A. F. Gibson, *J. Sci. Instrum.* **1958**, *35*, 273 – 278.

[10] F. Tuomisto, K. Saarinen, D. C. Look, G. C. Farlow, *Phys. Rev. B* **2005**, *72*, 085206.

Received: March 22, 2018
Version of record online June 19, 2018

